Int. j. adv. multidisc. res. stud. 2023; 3(1):744-753

Received: 18-12-2022
Accepted: 28-01-2023

International Journal of Advanced Multidisciplinary Research and Studies

ISSN: 2583-049X

Evaluation of the significant of thermal migration phenomenon on the reactive tiny particles micropolar flowing fluid past an elongated sheet

[1] TO Ogunbayo, [2] OA Esan, [3] AA Musilim, [4] MA Mohammed, [5] OE Enobabor, [6] OY Omikunle
[1, 2, 4, 5, 6] Department of Mathematics, Yaba College of Technology, Yaba, Nigeria
[3] Department of Welding and Fabrication Engineering, Yaba College of Technology, Yaba, Nigeria

Corresponding Author: **OA Esan**

Abstract
This article evaluates thermo-diffusion and diffusion-thermo effects on the motion of hydromagnetic reacting micropolar fluid along an elongated surface with lateral mass flux in porous media. This kind of study includes heat and mass transport of fluids which finds regular applications in various fields of engineering and sciences like porous pipe design, groundwater hydrology, brain blood flow, etc. This body of work also presents a report on thermophoretic phenomenon together with viscous dissipation and heat source. The model equations are firstly transformed from partial derivatives to ordinary ones by the use of some similarity quantities and subsequently tacked numerically. The nonlinearity of the involving equations has compelled the use of stable Runge-Kutta-Fehlberg approach with shooting technique to provide the needed solution. To emphasize and discuss the influence of the primary governing parameters impacting on the flow fields, a variety of graphs have been sketched out and discussed qualitatively. Verification of the numerical code with existing data in literature shows an excellent agreement as checked under limiting conditions and presented in the table. It is evidently shown that the material quantity causes the fluid motion to accelerate whereas the suction term reduces the speed of fluid. Both thermo-diffusion and diffusion-thermo strengthen the heat distribution in the system while the concentration profile declines with chemical reaction.

Keywords: Thermo-Diffusion, Diffusion-Thermo, Suction/Injection Velocity, Thermophoresis

1. Introduction

Studies combining heat and mass transport have received more attention from scholars in the recent years. This is because the presence of two species with distinct diffusivity in a system provides various useful convective relationship. Various applications of such can be found in the fields of engineering like geothermal reservoirs, metallurgical systems, groundwater movement of solutes substances, fibrous movement of air in an insulated material, etc [1-4]. Furthermore, the simultaneous transmission of mass and heat is common in both natural and man-made transport phenomena, and the joint buoyancy effects of thermal diffusion and chemical species diffusion cause it. As such, these techniques are used in industrial settings in fields like food processing, crop damage from freezing, the manufacturing of polymers, etc. [5-6].

A popular heat and mass transfer phenomenon is the thermo-diffusion also called Soret effect and diffusion-thermo also known to as Dufour effect. The thermo-diffusion is described as the concentration flux due to energy gradient; it is often in found fluid mechanics problems such as in situations of heat-mass transfer when the changes in density with temperature causes buoyancy effect in a free convection flow. At such occurrence the diffusion species is affected by temperature variation in the temperature. This phenomenon is applicable in separating and mixing gases with small molecular weight like hydrogen and helium. On the other hand, diffusion-thermo is the heat gradient resulting from concentration flux. These two quantities are of second order effect because it is believed that their magnitude is of smaller order in comparison to that of Fourier and Fick effects. However, these quantities are of crucial usefulness in practical engineering works such as geothermal energy, geosciences operations and chemical engineering activities and as such, they cannot be ignored. Various authors have included these phenomena due to applications, Postelnicu [7] assessed the transport of heat and mass due to free convection in a vertically expanding plate featuring the effects of Soret and Dufour whereas Tewfik *et al*. [8] investigated such phenomenon in an impermeable surface with various parameters. Kumar *et al*. [9] carried an analysis of the impact of radiation heat source on the flow of non-Newtonian fluid passing a plate of uneven thickness with the influence of Soret and Dufour using Homotopy analysis method. Other notable works on this concept can be found in Refs [10-12]. Thermophoresis is a phenomenon of movement of micro-particles in the direction declining heat gradient. In a such a situation the force accumulated by the tiny particles due to the heat gradient is called the thermophoresis force whereas the speed of the particles is known as thermophoretic velocity. Such concept is often encountered in manufacturing and engineering operations like in micro-contamination control, aerosol collection and so on. In the first investigation of this phenomenon, carried out by Goldsmith and May [13], the researchers investigated the prospect of a thermophoretic transport flow in a single dimension. Hayat *et al*. [14] reported on the effect of thermophoresis and haphazard motion of tiny particles of micropolar over a stretched plate with thermal radiation while Animasaun [15] evaluated thermophoresis and Dufour phenomenon on the motion of Casson fluid with nonuniform viscosity and thermal conductivity coupled with chemical reaction. More research works on this can be found in Refs [16-18]. Due to its numerous uses in gas turbines, nuclear power plants, electric transformers, etc., combined heat and mass transfer is a popular topic of study in science, engineering, and industrial operations. The movement of fluids through porous media has significant implications in various areas of science and technology due to the wide range of applications to which it is applicable such as dispersing chemical pollutants in saturated soil, groundwater hydrology, irrigation systems. Alam *et al*. [19] used numerical methods to establish local similarity solutions for the flow of an MHD micropolar fluid through a porous media, where they discovered that the skin friction coefficient decreases with increasing the Darcy parameter. Olajuwon *et al*. [20] employed the perturbation method to research the problem at concern and found that the Darcy and inertia factors were responsible for the decrease in the velocity field.

The term micropolar fluid refers to fluids with microstructures and stiff bar-like particles as part of their composition, Lukaszewicz [21]. As a result of the inherent microstructural properties of micropolar fluids, these fluids provide a good mathematical guideline for modeling and simulating complex and convoluted fluids, the likes of which cannot be effectively captured by the Navier-Stokes model. This is because micropolar fluids have a high dipole moment (Newtonian model). Fluids such as animal blood, colloids, liquid crystals, and so on are those that describe micropolar model [22-23]. So far, Eringen [24-25] is credited with having originated the theory of micropolar fluid, including the concept of thermo-micropolar fluid [26-27]. This model allows for the connection of microrotation and macro velocity fields, indicating microscopic action that causes the fluid element to translate and rotate simultaneously. In fact, the flow pattern of some fluids, such as liquid crystals, blood flows, suspension solutions, and other biological flows, might serve as a viable model for a micropolar fluid [28]. There are considerable uses of such fluids in engineering and industrial activities, for example, in the bio-mechanic and chemical engineering, extrusion of polymer, slurry technologies, synovial lubrication, arterial blood flows, and knee cap mechanics, to name just a few of many [29-30].

It is worthwhile to examine such a mathematical problem, particularly when one considers the vast number of applications that may be derived from research involving heat and mass movement under the impact of thermo-diffusion, diffusion-thermo, thermophoresis and chemical reactions. Therefore, this paper aims to explore the impact of Soret and Dufour with thermophoretic motion of a hydromagnetic micropolar fluid induced by an extending vertical plate in porous media. The model jointly combined the influence of viscous dissipation, thermal radiation and heat source in the heat profile. This research can potentially find applications in the fields of engineering like extraction of crude oil, groundwater hydrology, irrigation system and including medication administration and tissue transplant in bio-engineering.

2. Problem Design

With the assumption that the flow is time-independent, viscous and incompressible on a two-dimensional vertical plate in a porous device. It is assumed that Boussinesq approximation holds valid in the momentum equation. It is assumed that the working fluid is electro-conducting micropolar fluid which is both reactive and dissipative. The influence of thermo-diffusion, diffusion-thermo including thermophoresis plus thermal radiation holds in the model equation. No induced magnetic field but external one which is imposed in a transverse direction to the motion of the fluid as indicated in Fig 1. The micropolar boundary condition is taken to be weak concentration with $\alpha = 0.5$ whereas the expanded sheet speed is $\bar{U} = U_0$. The heat condition is believed to be isothermal ($T = T_s$) in nature with heat source included in the heat profile.

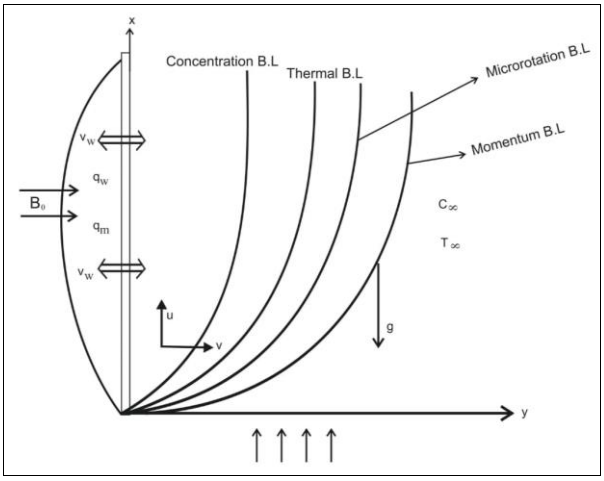

Fig 1: The Geometry of the Physical Model

Combining these assumptions stated above, with boundary layer approximation rule in place, then one can express the equation describing the problem as listed under;

$$\frac{\partial \bar{U}}{\partial x}+\frac{\partial \bar{V}}{\partial y}=0, \quad (1)$$

$$\bar{U}\frac{\partial \bar{U}}{\partial x}+\bar{V}\frac{\partial \bar{U}}{\partial y}=\frac{1}{\rho}(\mu+\beta)\frac{\partial^2 u}{\partial y^2}+\frac{\beta}{\rho}\frac{\partial N}{\partial y}+g\kappa_1(T-T_\infty)+g\kappa_2 C(C-C_\infty)-\frac{1}{\rho}\sigma B_0^2\bar{U}-\frac{\vartheta}{K}\bar{U}, \quad (2)$$

$$\bar{U}\frac{\partial N}{\partial x}+\bar{V}\frac{\partial N}{\partial y}=\frac{\Gamma}{\rho\xi}\frac{\partial^2 N}{\partial y^2}-\frac{\beta}{\rho\xi}\left(2N+\frac{\partial \bar{U}}{\partial y}\right), \quad (3)$$

$$\bar{U}\frac{\partial T}{\partial x}+\bar{V}\frac{\partial T}{\partial y}=\frac{K_r}{\rho C_P}\frac{\partial^2 T}{\partial y^2}+\frac{1}{\rho C_P}(\mu+\beta)\left(\frac{\partial \bar{U}}{\partial y}\right)^2+\frac{1}{\rho C_P}(T-T_\infty)+\frac{DmK_T}{\rho C_P Cs}\frac{\partial^2 C}{\partial \bar{y}^2}, \quad (4)$$

$$\bar{U}\frac{\partial C}{\partial \bar{y}}+\bar{V}\frac{\partial C}{\partial y}=Ds\frac{\partial^2 C}{\partial y^2}+\frac{DsK_T}{T_m}\frac{\partial^2 T}{\partial y^2}-K^*(C-C_\infty)-\frac{\partial}{\partial y}(V_T C) \quad (5)$$

The constraints at the wall are

$$\bar{U}(x,0)=U_0, \bar{V}(x,0)=V_w, N(x,0)=-\alpha\frac{\partial \bar{U}}{\partial y}, T(x,0)=T_s, C(x,0)=C_s$$
$$\bar{U}=0, N\to 0, T\to T_\infty, C\to C_\infty \;\; as \;\; y\to\infty. \quad (6)$$

Where $V_T=-\frac{k_t^*}{T_{ref}}\frac{\partial T}{\partial y}$ indicates thermophoresis velocity with $k_t^*=\frac{2Cs(\kappa/k_s+C_tK_n)(C_1+C_2e^{C_3/K_n})}{(1+3C_mK_n)(1+2\kappa/k_s+2C_tK_n)}$ indicating thermophoresis coefficient. More so, κ_1,κ_2,K^*, K,Ds,Cs and T_m respectively indicates thermal expansion coefficient, solutal expansion coefficient, rate of reaction, porous media permeability, mass diffusivity, susceptibility of the fluid, temperature of the mean fluid. In addition, $\bar{U}$ and $\bar{V}$ defines velocity components in the direction of x and y sequentially, $\mu,\vartheta,\beta,K_r,T,T_w,T_\infty,N,\rho$ describes dynamic viscosity, kinematic viscosity, vortex viscosity, thermal conductivity, temperature, wall temperature, free stream temperature, microrotation component, density respectively. Besides, specific heat is indicated by C_p, the spin gradient viscosity is symbolized with Γ, suction/injection speed is presented with V_w whereas the electric conductivity is expressed by σ, k_s indicates particles diffusion thermal conductivity, K_n defines the Knudsen number while α describes surface concentration of micropolar fluid which has the interval between 0 and 1. For similar solution to occur it is assumed in this study that $V_s=\frac{V_1}{x}, \sigma=\frac{\sigma_0}{x}, \kappa_1=\frac{\kappa_0}{x}, K^*=\frac{K_0}{x}, K=K_r x$ with $V_1,\sigma_0,\kappa_0,K_r,k_0$ being constants.

3. Similarity quantities

The stream functions $\bar{U}=\frac{\partial\psi}{\partial y}, \bar{V}=-\frac{\partial\psi}{\partial x}$ together with the similarity quantities and dimensionless quantities below are used to remodel the governing equations from partial to ordinary differential equations and thus reduce the independent variables to one.

$$\frac{\eta}{y}=\sqrt{\left(\frac{U_0x^{-1}\vartheta^{-1}}{2}\right)}, \psi=\sqrt{(2U_0x\vartheta)}f(\eta), N=U_0\sqrt{\left(\frac{U_0x^{-1}\vartheta^{-1}}{2}\right)}g(\eta), \Gamma=\left(\mu+\frac{\beta}{2}\right)\xi$$
$$\phi(\eta)=\frac{C-C_\infty}{C_s-C_\infty}, \theta(\eta)=\frac{T-T_\infty}{T_s-T_\infty}, fw=\sqrt{\frac{2V_0^2}{U_0\vartheta}}, M=\frac{2\sigma_0B_0^2}{\rho U_0}, Du=\frac{D_mK_T(C_s-C_\infty)}{Csc_p\vartheta(T_w-T_\infty)},$$
$$Gr=\frac{2g\beta_0(T_s-T_\infty)}{U_0^2}, Gc=\frac{2g\beta_0^*(C_s-C_\infty)}{U_0^2}, K=\frac{\beta}{\mu}, Ec=\frac{U_0^2}{cp(T_s-T_\infty)}, Pr=\frac{\mu C_p}{K_r},$$
$$Da=\frac{2\nu}{k_oU_0}, Sc=\frac{\nu}{Dm}, \delta=\frac{2k_1}{U_0}, Sr=\frac{DmK_T(T_s-T_\infty)}{T_m\vartheta(C_s-C_\infty)}, h=-\frac{k_t^*(T_s-T_\infty)}{T_0}. \quad (7)$$

Consequent upon using the similarity quantities above, there is satisfaction of the continuity equation and the other equations are transformed to the underlisted ordinary derivatives.

$$(1+K)\frac{d^3f}{d\eta^3}-(Da+M)\frac{df}{d\eta}+K\frac{dg}{d\eta}+f(\eta)\frac{d^2f}{d\eta^2}+Gr\theta(\eta)+Gc\phi(\eta)=0, \quad (8)$$

$$\left(1+\frac{K}{2}\right)\frac{d^2g}{d\eta^2}-2K\left(2g(\eta)+\frac{d^2f}{d\eta^2}\right)+\left(g\frac{df}{d\eta}+f\frac{dg}{d\eta}\right)=0, \quad (9)$$

$$(1+R)\frac{d^2\theta}{d\eta^2}+Prf\frac{d\theta}{d\eta}+Pr(1+K)Ec\left(\frac{d^2f}{d\eta^2}\right)^2+PrEc(M+Da)\left(\frac{df}{d\eta}\right)^2+PrDu\frac{d^2\phi}{d\eta^2}+PrB\theta=0, \quad (10)$$

$$\frac{d^2\phi}{d\eta^2}-Sc\left[\delta\phi-\left(f(\eta)-h\frac{d\theta}{d\eta}\right)\frac{d\phi}{d\eta}-(Sr-h\phi(\eta))\frac{d^2\theta}{d\eta^2}\right]=0, \quad (11)$$

subject to wall conditions given by:

$$\frac{df}{d\eta} = 1, f(\eta) = fw, g(\eta) = -\alpha \frac{d^2 f}{d\eta^2}, \theta(\eta) = 1, \phi(\eta) = 1 \ at \ \eta = 0$$
$$\frac{df}{d\eta} = 0, g(\eta) = 0, \theta(\eta) = 0, \phi(\eta) = 0 \ as \ \eta \to \infty. \quad (12)$$

The wall viscous drag popularly known as the skin friction coefficient, the heat gradient also called the Nusselt number and the solutal gradient known as Sherwood number are the quantities of engineering delight relevant in this study. They are orderly expressed as

$$S_x = \frac{H_w}{\rho u_w^2}, H_x = \frac{x q_w}{K_r(T_s - T_\infty)}, Sh_x = \frac{x q_m}{D_s(C_s - C_\infty)}, \quad (13)$$

The dimensionless form of these quantities are orderly expressed as

$$S_x = [1 + (1-\alpha)K] Re_x^{-0.5} \frac{d^2 f}{d\eta^2}, H_x = -Re_x^{0.5} \frac{d\theta}{d\eta}, Sh_x = -Re_x^{0.5} \frac{d\phi}{d\eta} \ at \ \eta = 0. \quad (14)$$

Where H_w, q_w and q_m respectively defines shear stress, heat flux and mass flux. The parameters indicated in the ordinary derivatives equations (8-11) include $K, M, fw, Ec, Da, h, \delta, R, B, Du, Gr, Sr$ and Gc which are material parameter, magnetic term, suction/injection, Eckert number, Darcy, thermophoresis, chemical reaction, radiation, heat source, Dufour, Grashof number, Soret number, and solutal Grashof number.

4. Solution Technique

The nonlinearity of the system of equations (8-11) subject to equation 12 has mandated the use of numerical method for the solution to the current problem. Thus, the solution has been sought by means of stable Runge-Kutta-Fehlberg method and coupled with shooting analysis. Using this method involves choosing a finite value of η and then translate system of equations (8-11) subject to (12) into a set of first order simultaneous equations. In this way, the BVP is reduced into IVP by applying the shooting method. The the initial conditions are also gotten and then the resultant set of equations is simultaneously solved by Runge-Kutta-Fehlberg scheme via Maple 2016. The comprehensive report on the use of this method can be found in many articles (see [38-39]). For the analysis, the selected values of the parameters involved are $M = Da = K = fw = 0.5$, $R = Ec = 0.2$, $Gr = 2.0$, $Gc = 1.0$, $Du = 0.6$, $Sr = 0.2$, $\alpha = 0.5$, $h = 2.0$, $\delta = 0.7$, $Pr = 0.72$, $Sc = 0.62$, $B = 0.10$. Unless stated otherwise on the figures. The verification of the accuracy of developed code is carried out by comparing the data obtained on S_{f_x} as well as that of Hu_x with some exciting data of [29] and [17] in the limiting constraints. Evidently shown in Table 1 is the report of the comparison which shows good agreement and hence verified the present result.

Table 1: Computed values of S_x and H_x for variations in Du and Sr as compared with [29] and [17]

Du	Sr	Rahman *et al.* [29]		Aurangzaib *et al.* [17]		Present	
		S_x	H_x	S_x	H_x	S_x	H_x
0.03	2.0	6.229	1.1565	6.2387	1.1519	6.2299	1.1565
0.04	1.6	6.149	1.1501	6.1608	1.1446	6.1506	1.1506
0.05	1.2	6.072	1.1428	6.0879	1.1358	6.0735	1.1428
0.08	0.8	6.001	1.1333	6.0232	1.1232	6.0022	1.1332
0.20	0.4	5.955	1.1157	5.9969	1.0965	5.95702	1.1157

5. Results and Discussion

There is need to point out the impact of the emerging parameters in transport profiles. Each of the parameters contributed significantly in the flow field as demonstrated by various graphs. Thus, this section describes the impact these parameters make on the velocity, heat profile, microrotation field and concentration profile using different graphs to illustrate their impact.

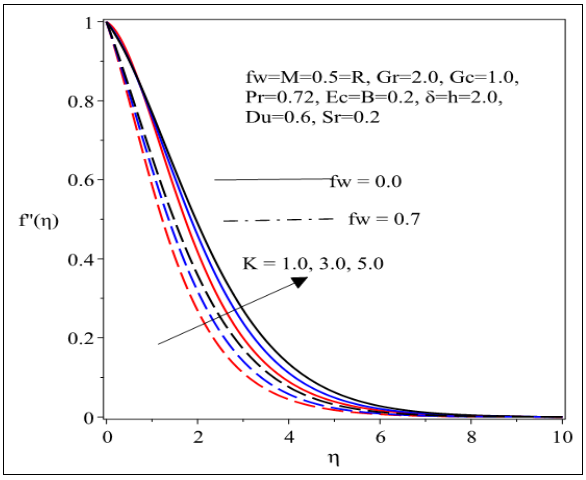

Fig 2: Influence of material term K on $f'(\eta)$

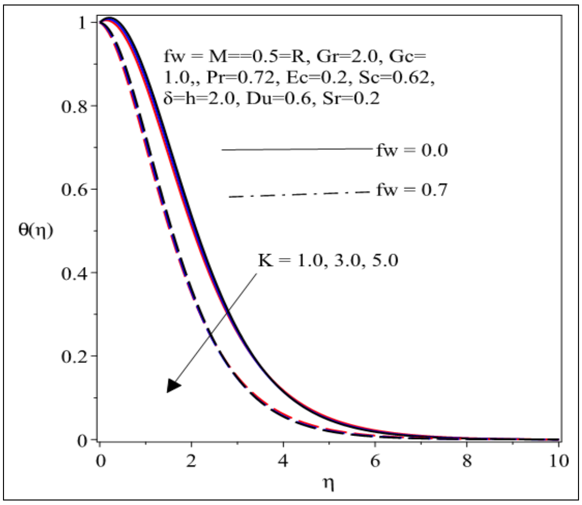

Fig 3: Impact of material term K on $\theta(\eta)$

There is an upward motion of the fluid for uplifting the material parameter K as indicated in Fig 2. An increase in K ($K = 1,3,5$) in the presence ($fw = 0.7$) or absence ($fw = 0$) of the lateral mass flux deplete the dynamic viscosity and thus breaking the resistance to the fluid movement, thereby a rise in the velocity profile $f'(\eta)$. More so, Fig 2 reveals that the motion of the fluid declines in the presence of suction term fw as compared to when fw is absent. However, the heat dissipation falls when the material term K increases as elucidated in Fig 3. Similarly, the presence of fw compels the surface temperature to fall together with the thermal boundary structure. The micropolarity of the fluid enhances the microrotation field to expand as K escalates as depicted in Fig 4.

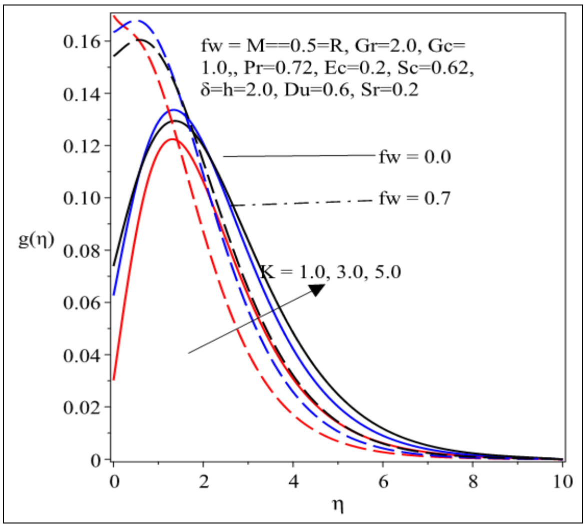

Fig 4: Variation of material term K on $g(\eta)$

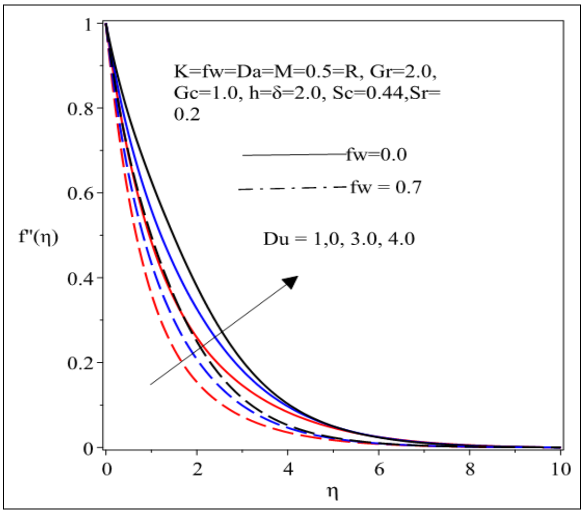

Fig 5: Reaction of Dufour term Du on $f'(\eta)$

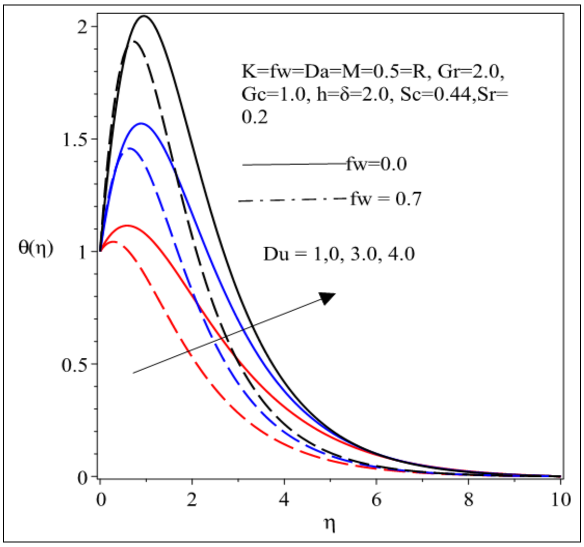

Fig 6: Reaction of Dufour term (Du) on $\theta(\eta)$

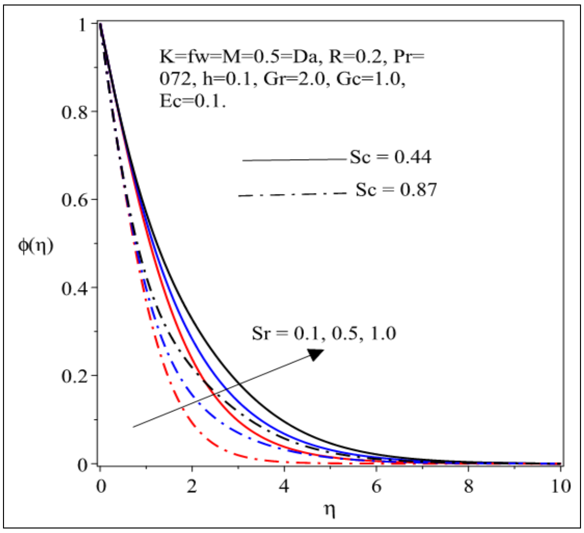

Fig 7: Impact of Soret Sr on $\phi(\eta)$

The presence of suction velocity raise the microrotation profile near the expanding wall whereas away from the wall there is a reduction in the microrotation profile as fw is imposed on the flow field. The velocity profile together with the hydrodynamic boundary film is stirred up by higher Dufour number as exemplified in Fig 5. A similar reaction occurs in the temperature region when the magnitude of Du is raised as found in Fig 6. This quantity Du describes the energy flux ratio due to the gradient of the concentration. More so, it is to be noted that Du is imposed in the heat equation of the current model where heat and mass motion are present and it is a second order function of solute substances. In view of this, a rise in Du induces the micropolar fluid tiny particles to generate more heat in the thermal field and then raises the thermal boundary thickness together with the surface temperature. However, the concentration field degenerates with growing values of the Schmidt number Sc because of the fact that there is lower molecular diffusivity when the value of Sc is raised but the presence of the Soret number boost the concentration field as demonstrated in Fig 7.

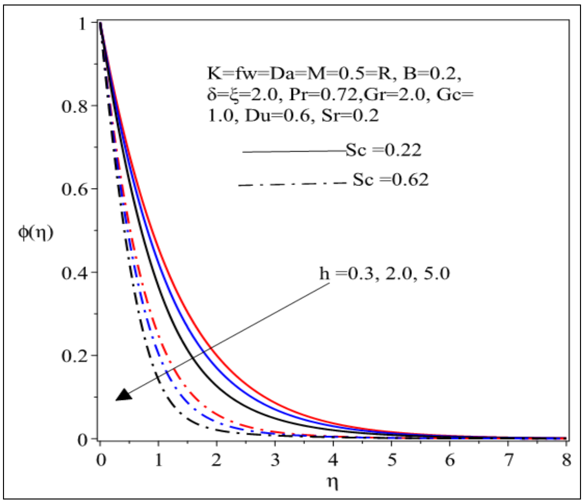

Fig 8: Impact of thermophoresis (h) on $\phi(\eta)$

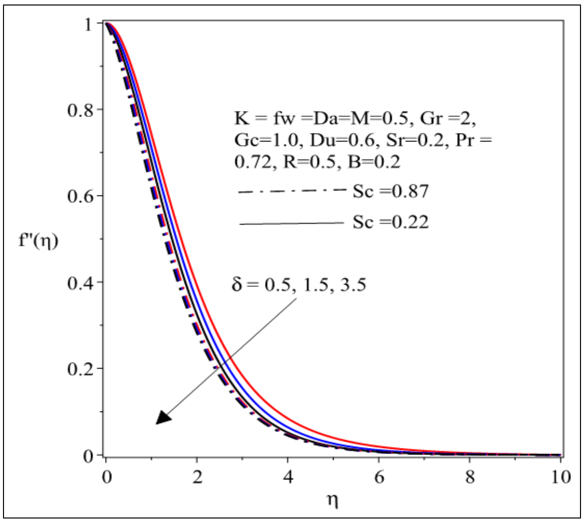

Fig 9: Effect of chemical reaction (δ) on $f'(\eta)$

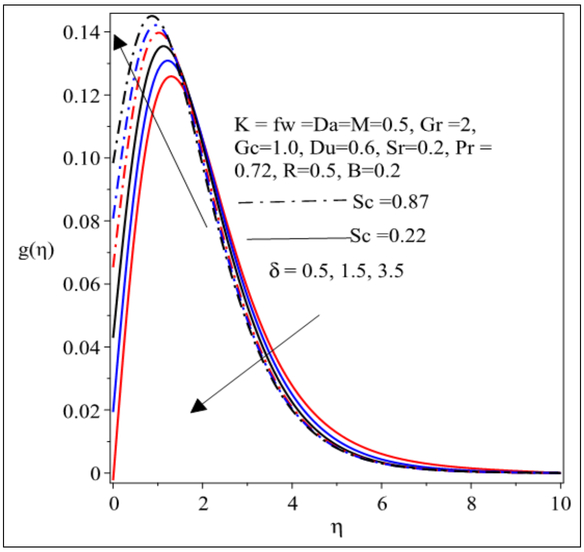

Fig 10: Impact of chemical reaction (δ) on $\phi(\eta)$

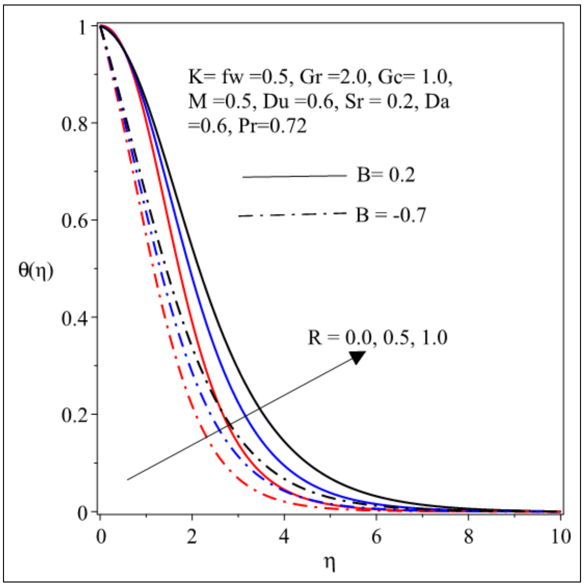

Fig 11: Influence of δ on $\phi(\eta)$

Meanwhile, it is observed in Fig 8 that thermophoresis parameter h degenerates the solutal boundary layer and thus reduce the concentration profile. This trend occurs because the micropolar fluid movement takes place form the hot region to the cold region and such phenomenon reduces the concentration profiles. It is thereby found that the impact of incorporating the thermophoretic term forces the concentration boundary layer film to shrink. Likewise, changes in the chemical reaction term δ leads to a fall in the velocity profiles and in the concentration profile as found in Fig 9 and 11 respectively in the presence of Sc.

There is shrink the solutal boundary layer field by raising the magnitude of both δ and Sc thereby causing a downward trend in the concentration field. Moreover, the microrotation field escalates near the expanding wall as δ increases but far from the wall there is a cross over situation and the trend is reversed as displayed in Fig 10. Fig 12 clearly elucidates the impact of the radiation term R as well as the heat generation B on the heat dissipation. Both parameters act to raise the temperature and compel the thermal boundary film to be thickened. However, the converse is the case for the Prandtl number Pr as found in Fig 13. There is a depleting thermal profile as Pr uplifts from 0.7, 1.5 and 3.0. The trend that occurs as a result of Pr is independent of heat generation presence as found in this figure.

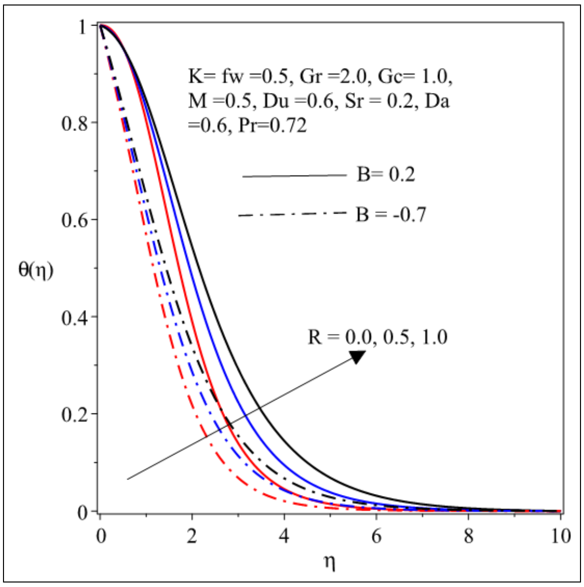

Fig 12: Impact of radiation term (R) on $\theta(\eta)$

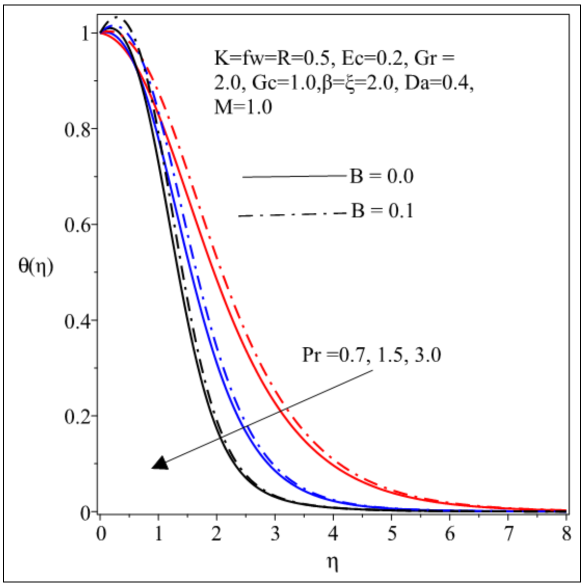

Fig 13: Effect of Prandtl number Pr on $\theta(\eta)$

6. Concluding remarks

The present article explores the impact of thermo-diffusion and diffusion-thermo with the thermophoretic flow of hydromagnetic micropolar fluid motion along and extending vertical plate in porous media. A two-dimensional sheet is investigated with heat and mass transfer incorporating thermal radiation, viscous dissipation and heat source in the energy profile. The main equations have been solved by means of Runge-Kutta Fehlberg method cum shooting technique and the solution is verified with earlier reported works in literature under some constraints and found to be in outstanding agreement. A variety of graphs have been sketched to unravel the significant contributions of the emerging parameters and deliberately qualitatively. The following points have been drawn from the study.

- There is a drastic decline in the fluid flow and heat dissipation by the imposition of suction term whereas an acceleration flow occurs with higher values of material term.
- A contracting thermal profile exists with higher Prandtl number whereas there is expansion in the thermal region when the thermal radiation and heat generation parameters increase in strength.
- There is contraction in the solutal boundary layer field due to a raise in the magnitude of the chemical reaction term, thermophoresis force and the Schmidt number thereby leading to a downward trend in the concentration profile
- An expansive hydrodynamic and thermal boundary film occurs with uplifting values of thermo-diffusion and diffusion-thermo parameters and consequently temperature and concentration profiles enhance due to these effects.

7. References

1. Israel-Cookey C, Amos E, Ebiwareme L. Soret and Magnetic Field Effects on Thermosolutal Convection in a Porous Medium with Concentration Based Internal Heat Source, American Journal of Fluid Dynamics. 2018; 8(2):41-46.
2. Gaikwad SN, Kamble SS. Analysis of linear stability on double diffusive convection in a fluid saturated anisotropic porous layer with Soret effect, Advances in Applied Science Research. 2012; 3(3):1611-1617.
3. Malshetty MS, Birador BS. The onset of double diffusive convection in a binary Maxwell fluid saturated porous layer with cross-diffusion effects. Physics of Fluids. 2011; 23; 064109:1-13.
4. Israel-Cookey C, Amos E. Soret and Radiation absorption effects on the onset of magneto-thermosolutal convection in a porous medium, Journal of Applied Mathematics and Bioinformatics. 2014; 4(1):71-87.
5. Pal D, Chatterjee S. Heat and mass transfer in MHD non-Darcian flow of a micropolar fluid over a stretching sheet embedded in a porous media with non-uniform heat source and thermal radiation. Commun Nonlinear Sci. Numer Simulat. 2010; 15:1843-1857.
6. Varol Oztop Y, Varol HF. Natural convection in porous triangular enclosures with a solid adiabatic fin attached to the horizontal wall International Communication in Heat and Mass Transfer. 2007; 34(1):19-27.
7. Postelnicu A. Influence of a magnetic field on heat and mass transfer by natural convection from vertical surfaces in porous media considering Soret and Dufour effects, International Journal of Heat and Mass Transfer. 2004; 47:1467-1472.
8. Tewfik OE, Eckert ERG, Jurewicz LS. Diffusion-thermo effects on heat transfer from a cylinder in cross flow, AIAA Journal. 1963; 1:1537-1543.
9. Kumar PV, Ibrahim SM, Lorenzini G. Thermal Radiation and Heat Source Effects on MHD Non-Newtonian Fluid Flow over a Slandering Stretching Sheet with Cross-Diffusion, Defect and Diffusion. 2018; 388:28-38.
10. Md. S Alam, Rahman MM. Dufour and Soret effects on MHD free convective heat and mass transfer flow past a vertical porous flat plate embedded in a porous medium, Journal of Naval Architecture and Marine Engineering. 2005; 1:55-65.
11. Aurangzaib ARM, Kasim NF, Shafie S. Soret and Dufour Effects on Unsteady MHD Flow of a Micropolar Fluid in the Presence of Thermophoresis Deposition Particle, World Applied Sciences Journal. 2013; 21(5):766-773.
12. Mishra SR, Baag S, Mohapatra DK. Chemical reaction and Soret effects on hydromagnetic micropolar fluid along a stretching sheet, Engineering Science and Technology, an International Journal. 2016; 19:1919-1928.

13. Goldsmith P, May FG. Diffusiophoresis and thermophoresis in water vapour systems, in: Aerosol Science, Academic Press, London, 1966.
14. Hayat T, Khan MI, Waqas M, Alsaedi A, Khan MI. Radiative flow of micropolar nanofluid accounting thermophoresis and Brownian moment, International Journal of Hydrogen Energy, 2017. http://dx.doi.org/10.1016/j.ijhydene.2017.05.006
15. Animasaun IL. Effects of thermophoresis, variable viscosity and thermal conductivity on free convective heat and mass transfer of non-Darcian MHD dissipative Casson fluid flow with suction and nth order of chemical reaction, Journal of the Nigerian Mathematical Society, 2014, 1-21.
16. Parida SK, Panda S, Rout BR. MHD boundary layer slip flow and radiative nonlinear heat transfer over a flat plate with variable fluid properties and thermophoresis. Alexandria Engineering Journal. 2015; 54:941-953.
17. Aurangzaib Md, Uddin S, Bhattacharyya K, Shafie S. Micropolar fluid flow and heat transfer over an exponentially permeable shrinking sheet, Propulsion and Power, 2016, 1-8.
18. Das K, Jana S, Kundu PK. Thermophoretic MHD Slip Flow over a permeable surface with variable fluid properties. Alexandria Engineering Journal, 2015; 35-44.
19. Alam MS, Ferdows M, Ota M, Maleque MA. Dufour and Soret effects on steady free convection and mass transfer flow past a semi-infinite vertical porous plate in a porous medium. Int J Appl Mech Eng. 2008; 11(3):535-545.
20. Olajuwon BI, Oahimire JI, Waheed MA. Convection heat and mass transfer in a hydromagnetic flow of a micropolar fluid over a porous medium. Theoret. Appl. Mech. 2014; 41(2):93-117.
21. Lukaszewicz G. Micropolar fluids: Theory and Applications (1st Ed.). Birkhauser, Boston. 1999; 33:1028-1031.
22. Fatunmbi EO, Odesola AS. MHD Free convective heat and mass transfer of a micropolar fluid flow over a stretching permeable sheet with constant heat and mass flux. Asian Research Journal of Mathematics. 2018; 9(3):1-15.
23. Salawu SO, Fatunmbi EO. Dissipative heat transfer of micropolar hydromagnetic variable electric conductivity fluid past inclined plate with Joule heating and non-uniform heat generation, Asian Journal of Physical and Chemical Sciences2017; 2(1):1-10.
24. Eringen AC. Theory of micropolar fluids. J. Math. Anal. Appl. 1966; 16:1-18.
25. Eringen AC. Theory of thermo-microfluids. Journal of Mathematical Analysis and Applications. 1972; 38:480-496.
26. Mohanty B, Mishra SR, Pattanayak HB. Numerical investigation on heat and mass transfer effect of micropolar fluid over a stretching sheet through porous media. Alexandria Engineering Journal. 2015; 54:223-232.
27. Fatunmbi EO, Fenuga OJ. MHD micropolar fluid flow over a permeable stretching sheet in the presence of variable viscosity and thermal conductivity with Soret and Dufour effects. International Journal of Mathematical Analysis and Optimization: Theory and Applications, 2017, 211-232.
28. Pal D, Mondal H. Effect of Soret Dufour, chemical reaction and thermal radiation on MHD non-Darcy unsteady mixed convective heat and mass transfer over a stretching sheet. Commun Nonlinear Sci Numer Simulat. 2014; 16:1942-1958. Doi: 10.1016/j.cnsns.2010.08.033
29. Rahman MM, Aziz A, Al-Lawatia MA. Heat transfer in micropolar fluid along an inclined permeable plate with variable fluid properties, Int. J of Thermal Sciences. 2010; 49:993-1002.
30. Mondal H, Pal D, Chatterjee S, Sibanda P. Thermophoresis and Soret-Dufour on MHD mixed convection mass transfer over an inclined plate with non-uniform heat source/sink and chemical reaction. Ain Shams Engineering Journal, 2017, 1-11.